View Online   Export Citation   CrossMark

Articles You May Be Interested In

Multi-wavelength lasing oscillation of a Vernier-type unidirectional Er 3+ -doped fiber compound ring

Appl. Phys. Lett. (June 1997)

Ultra-narrow linewidth dual-cavity opto-mechanical microwave oscillator based on radial guided acoustic modes of single-mode fiber

Appl. Phys. Lett. (January 2023)

Hybrid integrated external cavity laser with a 172-nm tuning range

APL Photonics (June 2022)
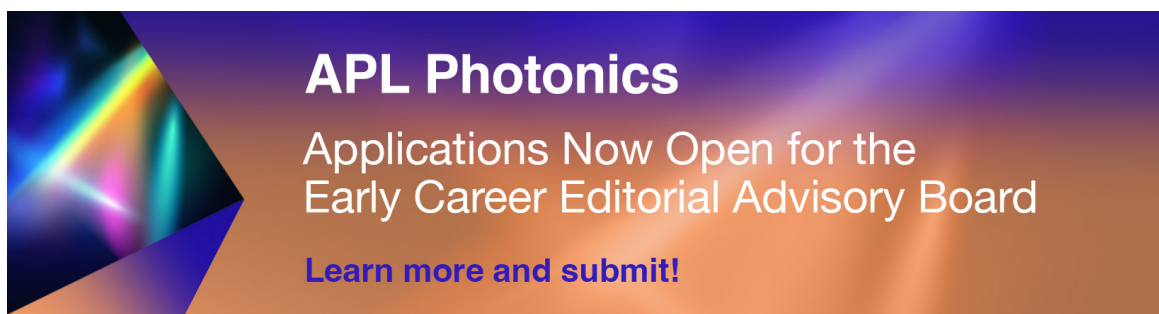
E-band widely tunable, narrow linewidth heterogeneous laser on silicon

View Online   Export Citation   CrossMark

Joel Guo,[a] (ID) Chao Xiang, (ID) Theodore J. Morin, (ID) Jonathan D. Peters, (ID) Lin Chang, and John E. Bowers[b] (ID)

AFFILIATIONS

Department of Electrical and Computer Engineering, University of California, Santa Barbara, California 93106, USA

[a] Author to whom correspondence should be addressed: joelguo@ucsb.edu
[b] Electronic mail: jbowers@ucsb.edu

ABSTRACT

We demonstrate a heterogeneously integrated laser on silicon exhibiting a sub-20 kHz Lorentzian linewidth over a wavelength tuning range of 58 nm from 1350 to 1408 nm, which are record values to date for E-band integrated lasers in the literature. Wide wavelength tuning is achieved with an integrated Si ring-resonator-based Vernier mirror, which also significantly reduces the Lorentzian linewidth. Such a record performance leverages a mature heterogeneous III–V/Si platform and marks an important milestone in E-band optical fiber communications and in reaching visible wavelengths via second harmonic generation for optical atomic clock applications.

I. INTRODUCTION

Historically, lasers operating in the telecommunication E-band (1360–1460 nm) have lagged in development due to the increased loss in optical fibers from water absorption.[1] With the development of dry fibers,[2] the optical attenuation in the E-band has fallen below that of the O-band. Subsequent work on E-band quantum dot lasers on GaAs substrates has renewed interest;[3] however, metamorphic buffers are required during growth, and coupling to low-loss waveguides for complex photonic circuitry, such as wavelength tuning and frequency noise reduction, has not been demonstrated.[4,5] Beyond optical communications, E-band lasers find usage in emerging visible spectrum applications by frequency doubling with integrated nonlinear photonics.[6,7] While direct emission lasers in the visible spectrum are being developed, they are also yet to demonstrate optical gain coupled to low-loss waveguides on a common substrate,[8–12] necessary to meet the linewidth and tuning requirements in atom-based applications.[13–15] Heterogeneous integration via wafer bonding addresses these issues on a scalable Si substrate, while allowing for wafer-level integration of nonlinear materials together with the laser pump source.[16–18] Here, we combine III–V optical gain and low-loss Si photonics and demonstrate a wide wavelength tunability of nearly 60 nm from 1350 to 1408 nm with Lorentzian linewidths below 20 kHz. We specifically target

wavelengths of 1396, 1378, and 1358 nm to address the 698 (clock), 689 (red MOT), and 679 nm (repump) wavelengths of a neutral strontium lattice clock.[13] Together with similar work in the O-band and S-C-L-bands, the heterogeneous Si photonics platform has demonstrated a spectral tuning range from 1238 to 1605 nm.[5,19–23] This range alone can cover nearly the entire spectral range of low-loss fiber communications. The device used in this work was co-processed together with heterogeneously integrated C-band lasers (requiring no additional processing steps), showing the feasibility of a tunable laser array covering the entire low-loss fiber communication spectral range on a single chip, as illustrated in Fig. 1. By augmenting with integrated second harmonic generation, this range can be extended to 600–800 nm for a host of visible light applications, such as atom-based clocks and quantum sensors.[13–15,24]

Figure 1(a) shows a schematic of the device. Optical gain is provided by the compressively strained aluminum gallium indium arsenide (AlGaInAs) multi-quantum well (MQW) gain material tailored for room temperature photoluminescence (PL) at 1370 nm and grown on a 3" indium phosphide (InP) wafer by a commercial vendor. This material was cleaved and bonded onto preprocessed Si waveguides, allowing for precise lithographic alignment of the InP and Si waveguides, as opposed to butt coupling of separate III–V and Si chips.[4] InP/Si tapered waveguide transitions and Si waveguides form the remainder of the cavity, with a Sagnac loop mirror and
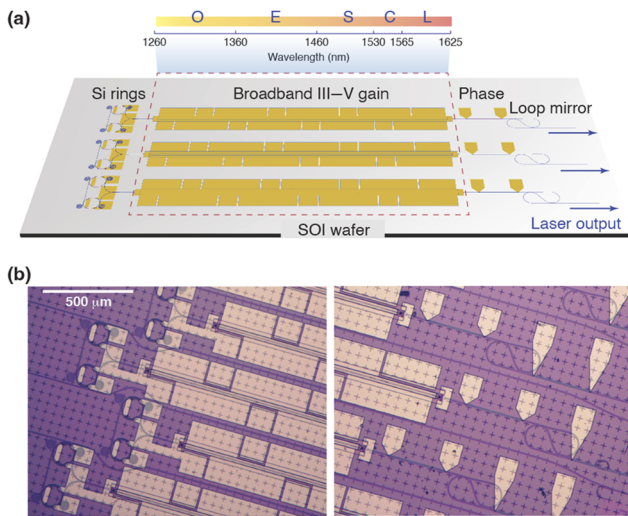
FIG. 1. Broadband tunable laser array concept covering the entire low-loss fiber telecommunication window. (a) Schematic of Si ring-resonator mirror lasers with the bonded III–V gain material in the O-band,[19–21] E-band (this work), and S-C-L-bands[5,22,23] on a common SOI wafer. The E-band laser used in this paper was co-processed together with C-band heterogeneous lasers on a common 100 mm Si substrate, demonstrating the feasibility of such a tunable laser array. (b) Microscope images of the ring resonators, phase shifters, and loop mirrors.

FIG. 2. Laser output power and wavelength tuning. (a) Fiber-coupled power and monotonically increasing wavelength tuning at 1396 nm with gain current. (b) Coarse wavelength tuning by individually sweeping each ring heater power.

phase section on one side of the gain and a ring-resonator-based mirror on the other side.[19–22] The two thermally tunable Si ring resonators are arranged in a Vernier configuration to simultaneously enable wide wavelength tunability and narrow instantaneous linewidth.[5] The MQW gain section is 2.4 mm long; the phase section heater is 300 μm long; and the ring resonator radii are 60 and 62 μm. The ring resonators are point coupled with a 340 nm gap between 650 nm wide bus and ring waveguides, resulting in ~5.8% cross-coupling [simulated via finite-difference time domain (FDTD)]. These resonators are likely undercoupled but will need to be confirmed by further waveguide loss investigation at these unconventional wavelengths. A 370 nm gap between the 650 nm wide waveguides in the Sagnac mirror results in a simulated reflection of about 8.6%. These relatively high mirror losses increase the threshold current, compared to previous designs at 1550 nm.[5] Optimized designs will favor a loop mirror reflectivity, yielding a higher output power over a reduced laser threshold for more second harmonic power with future nonlinear device integration.

The device was mounted on a temperature controlled stage and held at 20 °C. Holding the ring 1 heater power at 10.1 mW and the ring 2 heater power off, the gain current was swept, and the fiber-coupled power and wavelength were measured, as shown in Fig. 2(a). The aforementioned low Sagnac reflection and resultant loss from the undercoupled rings explains the high threshold current of 175 mA. Despite high mirror losses in this first demonstration, these devices still achieve a sufficient net gain for laser oscillation. With a better understanding of the waveguide loss around 1396 nm, narrower bus-coupling gaps can be optimized in future iterations to increase the coupling in the rings and in the Sagnac reflector, which
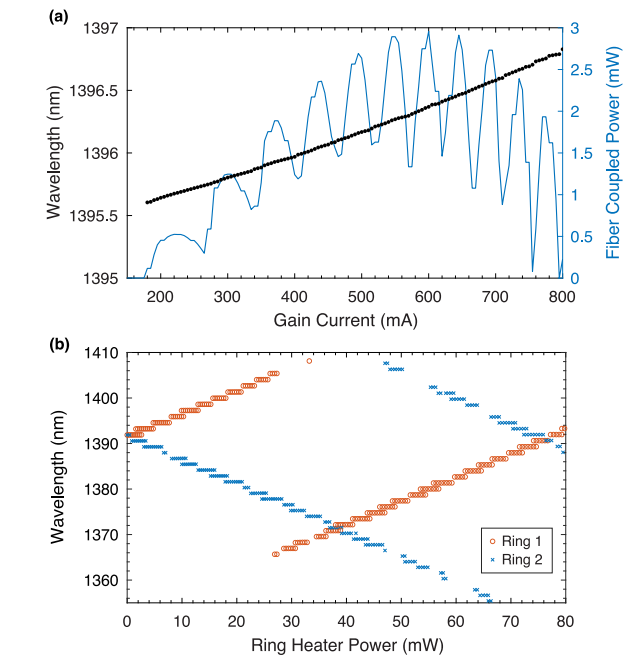
will reduce the total mirror loss and significantly improve the threshold, output power, side mode suppression ratio (SMSR), and laser linewidth. Assuming a low but reasonable loss of 1 dB/cm and ring coupling of 10%–20%, we expect to achieve lower threshold currents around 70 mA (accounting for the longer gain section used here) and output power exceeding 10 mW.[5]

A thermal roll-off is observed at around 600 mA and 3 mW fiber-coupled power, with a tuning range of over 1 nm around 1396 nm. ~6 dB fiber coupling loss gives over 10 mW on chip, which is comparable to output powers on similar devices in the O-band[20,21] and in the C-band,[22] albeit at a higher threshold and pump current. The dips in the power correspond to mode hops across adjacent longitudinal modes, and the small jumps in the corresponding wavelength (~15 pm) confirm the mode hops. However, due to the current tuning and mode hops both shifting the wavelength higher, increasing the gain current increases the wavelength monotonically. Furthermore, since the mode-hop-free tuning and mode hop steps are close within 10 pm (measured with a 1 pm resolution wavemeter), the tuning is effectively continuous, despite mode hops. Thus, when the rings are tuned appropriately, the gain current can be used as the frequency actuator in a Pound–Drever–Hall (PDH) locking scheme.[25] Tuning the ring resonators carefully can enable similarly monotonic wavelength tuning with gain current at the remaining target wavelengths. For continuous mode-hop-free tuning, the longitudinal cavity modes and Vernier ring modes must be aligned and tuned synchronously (via the gain or phase heater current and ring heater currents, respectively), adding tuning complexity.[26]

Figure 2(b) shows the broad wavelength tuning by sweeping each ring heater individually, while holding the gain current

constant at 350 mA. Coarse tuning in this manner covers a wide range of about 53 nm, from 1355 to 1408 nm. In both sweeps, the wavelength is shifted higher with increasing ring heater power; it then mode-hops higher for increasing ring 1 power and lower for increasing ring 2 power. Multi-mode lasing is observed near many mode hops and is attributed to undercoupled ring resonators and, thus, poor Vernier side mode suppression. This is mitigated by adjusting the intracavity phase with either the phase section heater or the gain current. Increasing the ring coupling strength with a smaller gap between the bus and ring waveguides can improve the Vernier side mode suppression, thus improving side-mode suppression at any given ring heater setting.[5] Multi-mode lasing and mode-hopping across adjacent Vernier modes (~40 nm separation) are observed at the edges of the tuning range, in which two adjacent Vernier modes tuned to either edge of the gain spectrum experience a comparable net gain. The difference between the two ring radii can be decreased such that the Vernier free spectral range (FSR) is slightly wider, thus ensuring that only a single Vernier mode is within the gain bandwidth at any ring heater configuration.[5] For both rings, around 75 mW is necessary to tune across a full Vernier FSR. A higher thermal tuning efficiency can be achieved with a thinner cladding between the Si waveguide and deposited heaters at the expense of metal absorption loss; alternatively, undercut Si waveguides can also be used for better thermal confinement.[27]

A tuning map and the selected optical spectra across the full tuning range are shown in Fig. 3. For the tuning map, both ring heaters are iteratively swept across a full Vernier FSR, while the gain current is held at 300 mA. Optical spectra are recorded at each step, and the dominant lasing wavelength is plotted as a function of heater power in Fig. 3(b).

Figure 3(a) shows the post-process-selected spectra at ~1 nm steps across a tuning range from 1350 to 1408 nm, all with a side mode suppression ratio (SMSR) above 50 dB. Such a tuning map can be used as a lookup table (LUT) to programmatically sweep across the tuning range of nearly 60 nm. A wider Vernier FSR design using rings with closer dimensions would enable even wider single mode tuning range, as the MQW gain bandwidth is greater than the Vernier FSR.[5] While the power variation is less than 10 dB, this can be reduced by optimizing the phase tuner to better align the longitudinal and ring modes.[22] The top panel in Fig. 3(a) shows the spectra from this work together with that of previous fully integrated tunable lasers demonstrated on the heterogeneous silicon photonics platform. With a laser array shown in Fig. 1(a), the majority of the low-loss fiber telecommunication spectral window can be covered on a single chip, with demonstrated tunability from 1238 to 1292 nm,[20] 1285 to 1330 nm,[21] 1350 to 1408 nm (this work), and 1490 to 1600 nm.[23] These tuning ranges were demonstrated with SMSRs greater than 45, 58, and 50 dB, respectively. Heterogeneously integrated lasers using micro-transfer-printing have also yielded impressive tuning ranges from 1495 to 1605 nm and 2305–2343 nm, both with a SMSR greater than 40 dB.[28,29]

Utilizing ring resonators not only allows for a wide tunability via the Vernier effect but also significantly enhances the effective cavity length at resonance, leading to a narrow Schawlow–Townes (Lorentzian) linewidth.[5] The Lorentzian linewidth can be calculated from the white noise floor of the frequency noise power spectral density (multiplied by π for double sideband PSD), which we extract here by averaging across the 20–100 MHz offset frequency range of
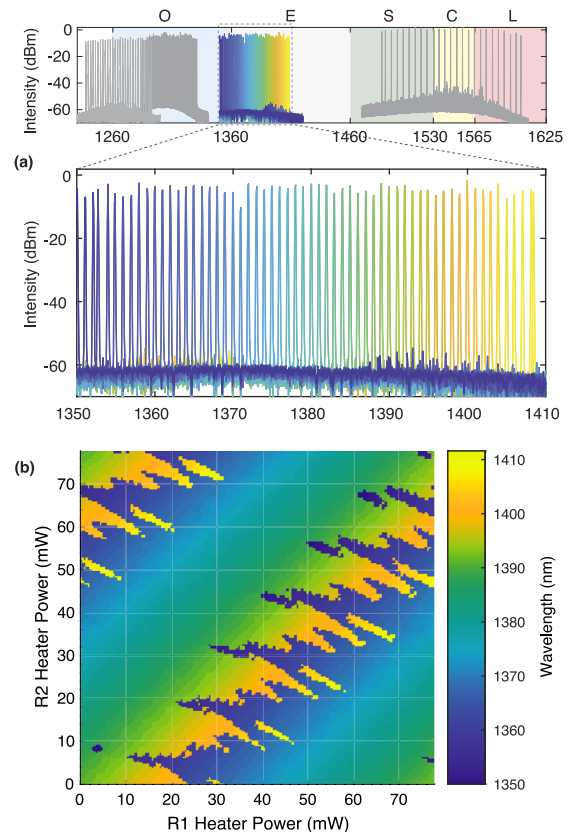
FIG. 3. Spectra across the tuning range and tuning map. (a) Optical spectra of the laser tuned from 1350 to 1408 nm with at least 50 dB SMSR, selected from the tuning map shown in (b). The top panel shows the spectra in this work together with that of similar tunable lasers on the heterogeneous silicon photonics platform, covering 1238–1292,[20] 1285–1330,[21] and 1490–1600 nm.[23] (b) 2D sweep of ring heater powers and the resultant lasing wavelengths extracted from the optical spectra taken at each operating point.

the frequency noise spectrum.[5] For these measurements, the ring heaters were manually tuned to achieve lasing across the entire tuning range and, then, the ring heaters and gain current were iteratively tuned to maximize the output optical power. Frequency noise was measured with a commercial optical phase noise analyzer (OEwaves OE4000) utilizing a quadrature-biased fiber Mach–Zehnder interferometer (MZI)-based frequency discriminator. Optical spectra were also taken at each point, yielding the SMSR. Frequency noise spectra for the four target wavelengths are shown in Fig. 4(a), with the dashed lines corresponding to white frequency noise floors. Technical (1/f) noise dominates at offset frequencies lower than 10 MHz, and packaging with designed electrical, thermal, and acoustic shielding would likely contribute to lower frequency noise at these offsets. Self-injection locking to a high-Q resonator dramatically reduces the frequency noise by >30 dB over an offset frequency range within the resonator bandwidth,[6,30] and such a resonator can be integrated together with the laser through wafer-bonding.[31,32] PDH-locking to a high-finesse cavity would further reduce the low-offset frequency noise within the servo bandwidth.[25,33]
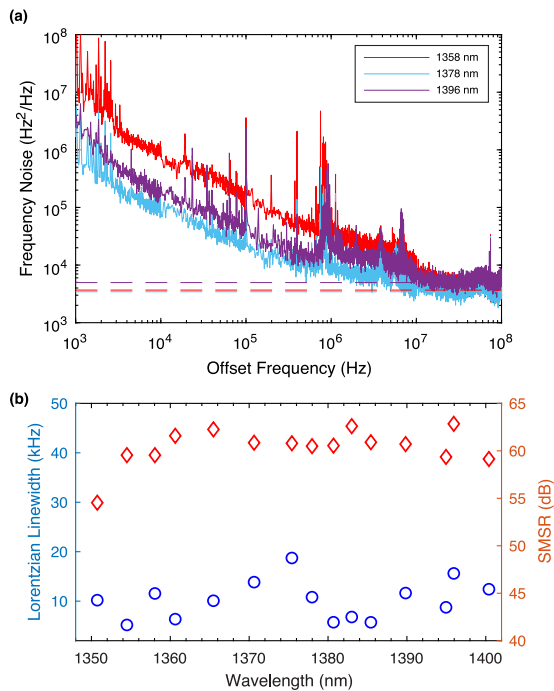
FIG. 4. Frequency noise spectrum and Lorentzian linewidth across the tuning range. (a) Frequency noise power spectral densities at the target lasing wavelengths of 1358, 1378, and 1396 nm. The dashed lines correspond to the white noise floors extracted to calculate the Lorentzian linewidth. (b) Lorentzian linewidths and SMSRs across the wavelength tuning range.

The Lorentzian linewidth is plotted with the lasing wavelength in Fig. 4(b), together with the SMSR from the corresponding optical spectrum. A Lorentzian linewidth of less than 20 kHz is demonstrated across the full tuning range, with SMSRs of 55 dB and above. To date, these are the narrowest Lorentzian linewidths and widest tuning range reported in the literature for E-band integrated lasers. In comparison, similar dual-resonator Vernier mirror-based lasers in the O-band and C-band have demonstrated linewidths in the range of 10–100 kHz[20,21,28] and sub-10 kHz.[22] Even narrower Lorentzian linewidths are straightforward to obtain with optimizations in the ring-resonator coupling to reduce mirror loss. Fabrication optimization, such as photoresist reflow to reduce waveguide surface roughness and scattering loss, would similarly help in improving the linewidth.

In conclusion, by combining commercially grown AlGaInAs/InP MQW material and low-loss Si ring-resonator-based Vernier mirrors, we demonstrate fully integrated, sub-20 kHz Lorentzian linewidth lasers across a tuning range of nearly 60 nm in the telecom E-band. These lasers were bonded and processed together with C-band lasers on the same 100 mm SOI wafer, and this approach can be taken to integrate tunable laser arrays covering the entire low-loss fiber telecom window on a single chip, which would greatly expand the spectral bandwidth of fiber-based communications applications. To fill in the gaps between tuning spectra in Fig. 3(a), the quantum well and barrier widths can be adjusted during growth to shift and flatten the gain spectrum; furthermore, multiple ring resonators can

be used to widen the Vernier FSR and, hence, the tuning range.[5] Because of the maturity of the heterogeneous III–V/Si platform and previous commercial demonstrations using different locally bonded gain materials for coarse wavelength division multiplexing, this work provides a realistic path toward high-volume manufacturing of such tunable lasers arrays.[34] With promising developments in integrated nonlinear photonics, these laser frequencies can be doubled via second harmonic generation to visible wavelengths relevant for atomic clocks.[6,7] With second harmonic conversion efficiencies in periodically poled lithium niobate (PPLN) reaching up to 50% and low coupling losses from heterogeneous integration, we expect several mW on chip in the second harmonic with the current design and over 10 mW with optimized mirror coupling.[31,35] By self-injection locking to a high-Q PPLN resonator, the second harmonic can be generated while simultaneously suppressing the frequency noise (determined by Q) and removing the need for an isolator between the pump laser and frequency converter. With a loaded Q of 400 k at the fundamental and 150 k at the second harmonic, such a PPLN self-injection locked configuration is capable of generating a second harmonic with a linewidth of 4.7 kHz.[6] Heterogeneous integration via wafer bonding provides a path for such nonlinear materials to be integrated together with these tunable laser arrays for fully integrated, narrow linewidth, visible light generation on a chip.[16,18] For long term stability and Hz-level integrated linewidths required for probing a strontium clock transition, further PDH-locking the fundamental to a high-finesse reference cavity is necessary.[33,36] Together with the tremendous progress in compact reference cavities for frequency stabilization and photonic integrated planar metasurfaces to cool, trap, and probe atomic species,[37,38] our work demonstrates a crucial component in the construction of a compact optical atomic clock for mobile, high-precision, GPS-free navigation applications.

AUTHOR DECLARATIONS
Conflict of Interest

The authors have no conflicts to disclose.

Author Contributions

Joel Guo: Conceptualization (supporting); Data curation (lead); Formal analysis (lead); Investigation (lead); Methodology (lead); Project administration (supporting); Software (lead); Validation (lead); Visualization (equal); Writing – original draft (lead); Writing – review & editing (lead). **Chao Xiang**: Investigation (equal); Methodology (equal); Project administration (equal); Supervision (equal); Writing – review & editing (supporting). **Theodore J. Morin**: Investigation (supporting); Writing – review & editing (equal). **Jonathan D. Peters**: Investigation (supporting); Methodology (equal); Resources (equal). **Lin Chang**: Project administration

(supporting); Resources (supporting); Supervision (supporting). **John E. Bowers**: Conceptualization (lead); Funding acquisition (lead); Project administration (lead); Supervision (lead); Writing – review & editing (supporting).

DATA AVAILABILITY

The data that support the findings of this study are available from the corresponding author upon reasonable request.

REFERENCES

[1] G. P. Agrawal, *Fiber-Optic Communication Systems* (John Wiley & Sons, 2012), Vol. 222.

[2] G. A. Thomas, B. I. Shraiman, P. F. Glodis, and M. J. Stephen, "Towards the clarity limit in optical fibre," Nature **404**, 262–264 (2000).

[3] J. Kwoen, T. Imoto, and Y. Arakawa, "InAs/InGaAs quantum dot lasers on multi-functional metamorphic buffer layers," Opt. Express **29**, 29378–29386 (2021).

[4] C. Xiang, W. Jin, D. Huang, M. A. Tran, J. Guo, Y. Wan, W. Xie, G. Kurczveil, A. M. Netherton, D. Liang, H. Rong, and J. E. Bowers, "High-performance silicon photonics using heterogeneous integration," IEEE J. Sel. Top. Quantum Electron. **28**, 8200515 (2022).

[5] M. A. Tran, D. Huang, and J. E. Bowers, "Tutorial on narrow linewidth tunable semiconductor lasers using Si/III-V heterogeneous integration," APL Photonics **4**, 111101 (2019).

[6] J. Ling, J. Staffa, H. Wang, B. Shen, L. Chang, U. A. Javid, L. Wu, Z. Yuan, R. Lopez-Rios, M. Li et al., "Self-injection locked frequency conversion laser," Laser Photonics Rev. (published online, 2023).

[7] M. Li, L. Chang, L. Wu, J. Staffa, J. Ling, U. A. Javid, S. Xue, Y. He, R. Lopez-Rios, T. J. Morin et al., "Integrated Pockels laser," Nat. Commun. **13**, 5344 (2022).

[8] T. Kamei, T. Kamikawa, M. Araki, S. P. DenBaars, S. Nakamura, and J. E. Bowers, "Research toward a heterogeneously integrated InGaN laser on silicon," Phys. Status Solidi A **217**, 1900770 (2020).

[9] A. Siddharth, T. Wunderer, G. Lihachev, A. S. Voloshin, C. Haller, R. N. Wang, M. Teepe, Z. Yang, J. Liu, J. Riemensberger et al., "Near ultraviolet photonic integrated lasers based on silicon nitride," APL Photonics **7**, 046108 (2022).

[10] M. Corato-Zanarella, A. Gil-Molina, X. Ji, M. C. Shin, A. Mohanty, and M. Lipson, "Widely tunable and narrow-linewidth chip-scale lasers from near-ultraviolet to near-infrared wavelengths," Nat. Photonics **17**, 157 (2022).

[11] N. Chauhan, A. Isichenko, K. Liu, J. Wang, Q. Zhao, R. O. Behunin, P. T. Rakich, A. M. Jayich, C. Fertig, C. W. Hoyt, and D. J. Blumenthal, "Visible light photonic integrated Brillouin laser," Nat. Commun. **12**, 4685 (2021).

[12] M. A. Tran, C. Zhang, T. J. Morin, L. Chang, S. Barik, Z. Yuan, W. Lee, G. Kim, A. Malik, Z. Zhang et al., "Extending the spectrum of fully integrated photonics to submicrometre wavelengths," Nature **610**, 54 (2022).

[13] M. M. Boyd, "High precision spectroscopy of strontium in an optical lattice: Towards a new standard for frequency and time," Ph.D. thesis, University of Colorado at Boulder, 2007.

[14] A. D. Ludlow, M. M. Boyd, J. Ye, E. Peik, and P. O. Schmidt, "Optical atomic clocks," Rev. Mod. Phys. **87**, 637 (2015).

[15] G. Moody, V. J. Sorger, P. W. Juodawlkis, D. J. Blumenthal, W. Loh, C. Sorace-Agaskar, A. E. Jones, K. C. Balram, J. C. F. Matthews, A. Laing, M. Davanco, L. Chang, J. E. Bowers, N. Quack, C. Galland, I. Aharonovich, M. A. Wolff, C. Schuck, N. Sinclair, M. Loncar, T. Komljenovic, D. Weld, S. Mookherjea, S. Buckley, M. Radulaski, S. Reitzenstein, G. S. Agarwal, B. Pingault, B. Machielse, D. Mukhopadhyay, A. Akimov, A. Zheltikov, K. Srinivasan, W. Jiang, T. P. McKenna, J. Lu, H. X. Tang, A. H. Safavi-Naeini, S. Steinhauer, A. W. Elshaari, V. Zwiller, P. S. Davids, N. Martinez, M. Gehl, J. Chiaverini, K. K. Mehta, J. Romero, N. B. Lingaraju, A. M. Weiner, D. Peace, R. Cernansky, M. Lobino, E. Diamanti, R. M. Camacho, and L. Trigo Vidarte, "Roadmap on integrated quantum photonics," J. Phys.: Photonics **4**, 012501 (2021).

[16] C. Xiang, J. Liu, J. Guo, L. Chang, R. N. Wang, W. Weng, J. Peters, W. Xie, Z. Zhang, J. Riemensberger et al., "Laser soliton microcombs heterogeneously integrated on silicon," Science **373**, 99–103 (2021).

[17] C. Op de Beeck, F. M. Mayor, S. Cuyvers, S. Poelman, J. F. Herrmann, O. Atalar, T. P. McKenna, B. Haq, W. Jiang, J. D. Witmer et al., "III/V-on-lithium niobate amplifiers and lasers," Optica **8**, 1288–1289 (2021).

[18] W. Xie, C. Xiang, L. Chang, W. Jin, J. Peters, and J. E. Bowers, "Silicon-integrated nonlinear III-V photonics," Photonics Res. **10**, 535–541 (2022).

[19] T. Komljenovic, L. Liang, R.-L. Chao, J. Hulme, S. Srinivasan, M. Davenport, and J. E. Bowers, "Widely-tunable ring-resonator semiconductor lasers," Appl. Sci. **7**, 732 (2017).

[20] T. Komljenovic, S. Srinivasan, E. Norberg, M. Davenport, G. Fish, and J. E. Bowers, "Widely tunable narrow-linewidth monolithically integrated external-cavity semiconductor lasers," IEEE J. Sel. Top. Quantum Electron. **21**, 214–222 (2015).

[21] A. Malik, J. Guo, M. A. Tran, G. Kurczveil, D. Liang, and J. E. Bowers, "Widely tunable, heterogeneously integrated quantum dot O-band lasers on silicon," Photonics Res. **8**, 1551–1557 (2020).

[22] M. A. Tran, D. Huang, J. Guo, T. Komljenovic, P. A. Morton, and J. E. Bowers, "Ring-resonator based widely-tunable narrow-linewidth Si/InP integrated lasers," IEEE J. Sel. Top. Quantum Electron. **26**, 1500514 (2019).

[23] P. A. Morton, C. Xiang, J. Khurgin, C. D. Morton, M. A. Tran, J. D. Peters, J. Guo, M. J. Morton, and J. E. Bowers, "Integrated coherent tunable laser (ICTL) with ultra-wideband wavelength tuning and sub-100 Hz Lorentzian linewidth," J. Lightwave Technol. **40**, 1802 (2021).

[24] R. J. Niffenegger, J. Stuart, C. Sorace-Agaskar, D. Kharas, S. Bramhavar, C. D. Bruzewicz, W. Loh, R. T. Maxson, R. McConnell, D. Reens et al., "Integrated multi-wavelength control of an ion qubit," Nature **586**, 538–542 (2020).

[25] L. Stern, W. Zhang, L. Chang, J. Guo, C. Xiang, M. A. Tran, D. Huang, J. D. Peters, D. Kinghorn, J. E. Bowers, and S. B. Papp, "Ultra-precise optical-frequency stabilization with heterogeneous III–V/Si lasers," Opt. Lett. **45**, 5275–5278 (2020).

[26] P. Pintus, J. Guo, W. Jin, M. A. Tran, J. Peters, C. Xiang, J. Liang, O. J. Ohanian, and J. E. Bowers, "225 GHz mode-hop-free tuning with a narrow linewidth integrated InP/Si laser," in 2022 Conference on Lasers and Electro-Optics (CLEO) (IEEE, 2022), pp. 1–2.

[27] P. Pintus, M. Hofbauer, C. L. Manganelli, M. Fournier, S. Gundavarapu, O. Lemonnier, F. Gambini, L. Adelmini, C. Meinhart, C. Kopp et al., "PWM-driven thermally tunable silicon microring resonators: Design, fabrication, and characterization," Laser Photonics Rev. **13**, 1800275 (2019).

[28] E. Soltanian, G. Muliuk, S. Uvin, D. Wang, G. Lepage, P. Verheyen, J. Van Campenhout, S. Ertl, J. Rimböck, N. Vaissiere et al., "Micro-transfer-printed narrow-linewidth III-V-on-Si double laser structure with a combined 110 nm tuning range," Opt. Express **30**, 39329–39339 (2022).

[29] R. Wang, S. Sprengel, A. Vasiliev, G. Boehm, J. Van Campenhout, G. Lepage, P. Verheyen, R. Baets, M.-C. Amann, and G. Roelkens, "Widely tunable 2.3 µm III-V-on-silicon vernier lasers for broadband spectroscopic sensing," Photonics Res. **6**, 858–866 (2018).

[30] B. Li, W. Jin, L. Wu, L. Chang, H. Wang, B. Shen, Z. Yuan, A. Feshali, M. Paniccia, K. J. Vahala, and J. E. Bowers, "Reaching fiber-laser coherence in integrated photonics," Opt. Lett. **46**, 5201–5204 (2021).

[31] C. Xiang, W. Jin, J. Guo, J. D. Peters, M. J. Kennedy, J. Selvidge, P. A. Morton, and J. E. Bowers, "Narrow-linewidth III-V/Si/Si3N4 laser using multilayer heterogeneous integration," Optica **7**, 20–21 (2020).

[32] C. Xiang, J. Guo, W. Jin, L. Wu, J. Peters, W. Xie, L. Chang, B. Shen, H. Wang, Q.-F. Yang et al., "High-performance lasers for fully integrated silicon nitride photonics," Nat. Commun. **12**, 6650 (2021).

[33] J. Guo, C. A. McLemore, C. Xiang, D. Lee, L. Wu, W. Jin, M. Kelleher, N. Jin, D. Mason, L. Chang et al., "Chip-based laser with 1-hertz integrated linewidth," Sci. Adv. **8**, eabp9006 (2022).

[34] R. Jones, P. Doussiere, J. B. Driscoll, W. Lin, H. Yu, Y. Akulova, T. Komljenovic, and J. E. Bowers, "Heterogeneously integrated inp\/silicon photonics: Fabricating fully functional transceivers," IEEE Nanotechnol. Mag. **13**, 17–26 (2019).

[35] J. Y. Chen, C. Tang, M. Jin, Z. Li, Z. Ma, H. Fan, S. Kumar, Y. M. Sua, and Y. P. Huang, "Efficient frequency doubling with active stabilization on chip," Laser Photonics Rev. **15**, 2100091 (2021).

[36] C. A. McLemore, N. Jin, M. L. Kelleher, J. P. Hendrie, D. Mason, Y. Luo, D. Lee, P. Rakich, S. A. Diddams, and F. Quinlan, "Miniaturizing ultrastable electromagnetic oscillators: Sub-10−14 frequency instability from a centimeter-scale Fabry-Perot cavity," Phys. Rev. Appl. **18**, 054054 (2022).

[37] C. Ropp, A. Yulaev, D. Westly, G. Simelgor, and V. Aksyuk, "Meta-grating out-couplers for optimized beam shaping in the visible," Opt. Express **29**, 14789–14798 (2021).

[38] C. Ropp, W. Zhu, A. Yulaev *et al.*, "Integrating planar photonics for multi-beam generation and atomic clock packaging on chip," Light Sci. Appl. **12**, 83 (2023).